SMC-TR-92-45

AEROSPACE REPORT NO.
TR-0091(6945-01)-3

Modeling Performance Degradation in Nickel Hydrogen Cells

Prepared by

L. H. THALLER and T. P. BARRERA
Electronics Technology Center
Technology Operations

1 May 1991

Prepared for

SPACE AND MISSILE SYSTEMS CENTER
(formerly Space Systems Division)
AIR FORCE MATERIEL COMMAND
Los Angeles Air Force Base
P. O. Box 92960
Los Angeles, CA 90009-2960

Engineering and Technology Group

THE AEROSPACE CORPORATION
El Segundo, California

This report was submitted by The Aerospace Corporation, El Segundo, CA 90245-4691, under Contract No. F04701-88-C-0089 with the Space and Missile Systems Center, P. O. Box 92960, Los Angeles, CA 90009-2960. It was reviewed and approved for The Aerospace Corporation by B. K. Janousek, Principal Director, Electronics Technology Center. Paul M. Propp was the project officer for the Mission-Oriented Investigation and Experimentation (MOIE) program.

This report has been reviewed by the Public Affairs Office (PAS) and is releasable to the National Technical Information Service (NTIS). At NTIS, it will be available to the general public, including foreign nationals.

This technical report has been reviewed and is approved for publication. Publication of this report does not constitute Air Force approval of the report's findings or conclusions. It is published only for the exchange and stimulation of ideas.

QUANG BUI, Lt, USAF
MOIE Program Manager

PAUL M. PROPP
Wright Lab West Coast Office

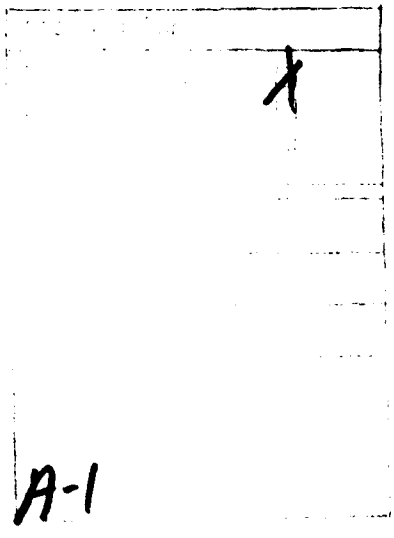

UNCLASSIFIED

URITY CLASSIFICATION OF THIS PAGE

REPORT DOCUMENTATION PAGE

REPORT SECURITY CLASSIFICATION Unclassified	1b. RESTRICTIVE MARKINGS
SECURITY CLASSIFICATION AUTHORITY	3. DISTRIBUTION/AVAILABILITY OF REPORT Approved for public release; distribution unlimited
DECLASSIFICATION/DOWNGRADING SCHEDULE	
ERFORMING ORGANIZATION REPORT NUMBER(S) TR-0091(6945-01)-3	5. MONITORING ORGANIZATION REPORT NUMBER(S) SMC-TR-92-45
NAME OF PERFORMING ORGANIZATION The Aerospace Corporation Technology Operations 6b. OFFICE SYMBOL *(If applicable)*	7a. NAME OF MONITORING ORGANIZATION Space and Missile Systems Center
ADDRESS *(City, State, and ZIP Code)*	7b. ADDRESS *(City, State, and ZIP Code)* Los Angeles Air Force Base Los Angeles, CA 90009-2960
NAME OF FUNDING/SPONSORING ORGANIZATION 8b. OFFICE SYMBOL *(If applicable)*	9. PROCUREMENT INSTRUMENT IDENTIFICATION NUMBER F04701-88-C-0089
ADDRESS *(City, State, and ZIP Code)*	10. SOURCE OF FUNDING NUMBERS PROGRAM ELEMENT NO. / PROJECT NO. / TASK NO. / WORK UNIT ACCESSION NO.

TITLE *(Include Security Classification)*

Modeling Performance Degradation in Nickel Hydrogen Cells

PERSONAL AUTHOR(S)
Thaller, Lawrence H. and Barrera, Thomas P.

TYPE OF REPORT	13b. TIME COVERED	14. DATE OF REPORT *(Year, Month, Day)*	15. PAGE COUNT
	FROM _____ TO _____		21

SUPPLEMENTARY NOTATION

COSATI CODES		
FIELD	GROUP	SUB-GROUP

18. SUBJECT TERMS *(Continue on reverse if necessary and identify by block number)*
Nickel hydrogen
Performance degradation
Life prediction models
Nickel electrode expansion

ABSTRACT *(Continue on reverse if necessary and identify by block number)*

With the increasing use of nickel hydrogen cells and batteries, degradation models and cycle life predictions can be valuable if they are valid. This report reviews previous studies of the expansion characteristics of nickel electrodes, as well as early efforts to predict cycle life as a function of depth of discharge. The results of these earlier studies are then used to suggest a more accurate degradation model for nickel electrodes. Preliminary experimental studies have focused on electrodes of the type used in typical flight hardware. The objective is to explore the stiffness of electrodes as they are cycled to different depths of discharge and different concentrations of KOH. Electrodes of different plaque strengths, loading levels of active material, and amounts of cobalt additives will eventually be investigated. The ultimate goal is to more accurately predict the cycle life of a cell as affected by design parameters.

DISTRIBUTION/AVAILABILITY OF ABSTRACT UNCLASSIFIED/UNLIMITED ☐ SAME AS RPT. ☐ DTIC USERS	21. ABSTRACT SECURITY CLASSIFICATION Unclassified
NAME OF RESPONSIBLE INDIVIDUAL	22b. TELEPHONE *(Include Area Code)* / 22c. OFFICE SYMBOL

FORM 1473, 84 MAR — 83 APR edition may be used until exhausted. All other editions are obsolete

SECURITY CLASSIFICATION OF THIS PAGE

UNCLASSIFIED

CONTENTS

FIGURES

1. INTRODUCTION

Nickel hydrogen cells are becoming a more important factor in the storage of electrical energy for aerospace applications. To date, many geosynchronous applications have successfully demonstrated the usefulness of these advanced batteries. The Hubble Space Telescope was the first large user of this newer technology in a low earth orbit application, but other uses are currently in the planning stage. Based on the results of cycle life testing, it is generally conceded that the expansion characteristics of nickel electrodes ultimately limit their useful lives. This report explores certain aspects of this phenomenon by first reviewing some of the more important past works addressing the structural properties of nickel electrodes and presenting a summary of representative cycle life results that have recently become available. This information is then used to update an earlier cycle life model that was based on the simple wear-out of the electrochemical components within a cell. Attempts to validate this updated model by adapting an existing experimental technique are then reviewed. In particular, the possible explanation for increased cycle life associated with nickel hydrogen cells using 26% KOH rather than the usual concentrations of either 31% or 36% KOH is examined.

A. Background

When nickel electrodes are prepared for use in nickel hydrogen cells, the void space within the nickel sinter is typically impregnated to the point of being half filled with active material. The exact value depends on the porosity of the plaque to be impregnated, which is close to 80%; the loading level of active material, which can range from 1.6 to 1.8 g of active material per cubic centimeter of void volume within the plaque; and, finally, the density of the active material, which is about 4.0 g/cm^3. Different manufacturers have preferred values for the plaque porosity and the loading level of active material. Although subject to variability depending on their exact morphological structure and degree of hydration, the densities as presented by Oshitani et al. are typical for these materials in KOH solutions (Ref.1). The values are as follows: beta NiOOH = 4.68g/cm^3, gamma NiOOH = 3.79 g/cm^3, alpha $Ni(OH)_2$ = 2.82g/cm^3, and beta $Ni(OH)_2$ = 3.97 g/cm^3. The fact that repeated cycling of the electrode can result in increases in the overall thickness of the electrode by up to 80%, as reported by Lim, is not clearly understood (Ref. 2). There has been increased interest in understanding this characteristic for obvious reasons, and this has taken research efforts in several separate directions. The analyses of structures (lattice constants, phase stabilities, etc.) as well as the physical study of electrode plate material (strength, swelling, etc.) have been carried out with emphasis placed on the effects of additives, electrolyte concentration, and loading level of active material. Selected references to these studies are examined in more detail in later sections of this report. The understanding of these factors should result in the development of life prediction models that would be of use in suggesting the cycling capability of a given cell design.

B. Previous Cycle-Life Model

Thaller and Lim reviewed existing cycle life information covering several secondary cell technologies and fitted it to an existing model for predicting cycle life as a function of depth of discharge (Ref. 3). The existing model was based on a simple wear-out type of failure (Ref. 4). In the simple wear-out model, a cell is assumed to be properly designed, assembled, and filled with electrolyte. Generally speaking, manufacturers incorporate extra capacity over and above the nameplate capacity to make up for gradual losses over cell usage. This value can range from 5% to 30% of the nameplate rating. When being cycled to a fractional depth of discharge, D, the excess capacity at the beginning of life is the sum of the uncycled capacity based on the nameplate value plus the reserve capacity. Figure 1 illustrates these values and definitions more clearly. This model assumes that there is a parameter, A, which determines the rate of capacity loss during the cycling. The numerical value of A is dependent on the particular cell chemistry and design factors. The capacity lost each cycle is the product of A and D, the fractional depth of discharge (DOD). As long as the original excess capacity can supply D ampere hours of capacity, the cell will continue to cycle. Mathematically, the cycle life, L, of a cell of normalized capacity (equal to 1.00), with a 20% excess capacity over and above the nameplate value, when cycled to the fractional DOD, D, will be:

$$L = (1-D + 0.2)/A*D \qquad (1)$$

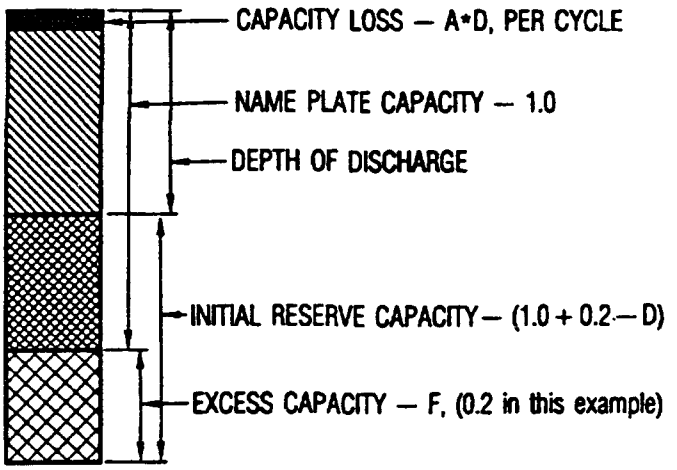

Figure 1. Cell capacity diagram

The general shape of the cycle life/DOD relationship is depicted in Figure 2. If there had been no excess capacity over and above the nameplate value, the curve would have decreased much more rapidly at the deeper DODs. By changing the value of A, the parameter that determines the rate of capacity loss, the curve would shift as a simple translation of the curve shown in Figure 2. The middle portion of the curve is nearly straight and would predict a doubling of cycle life for every 20% reduction in DOD. This is in general agreement with results for life cycle testing. This doubling is not a consequence of a selected value of A, but rather a consequence of wear-out as the failure mechanism.

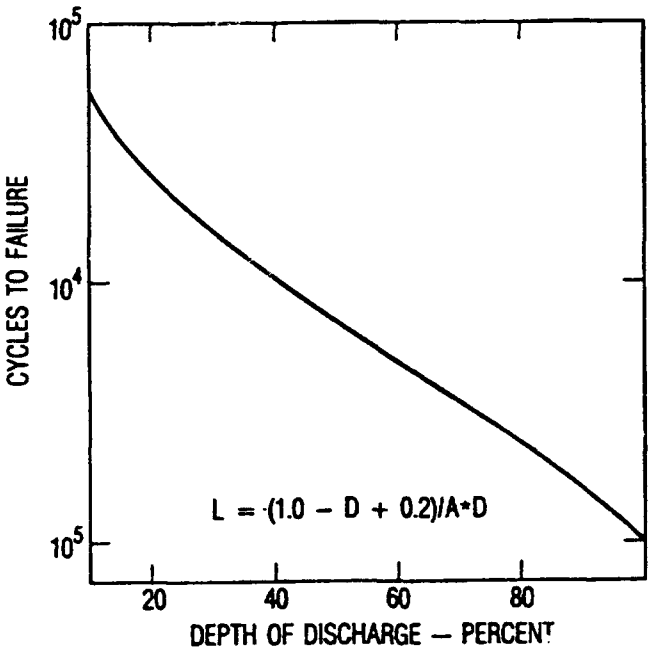

Figure 2. Cycle life prediction using simple wear-out model

In the 1987 report of Thaller and Lim, cycle life data from several different cell chemistries were collected (Ref. 3). These data were felt to represent the upper limits of what one could expect from these different types of cells. Some of these data came from experimental cells, some from boiler plate articles, and some from early production runs. The 2505 nickel cadmium data came from a Crane report of some early standard-weight cells that NASA was testing (Ref. 5). The Super Nicad data came from in-house company funded work at the Hughes Research Laboratory, and the nickel hydrogen data came from NASA funded studies at the Hughes Research Laboratory (Ref. 6). Figure 3 supports the suggestion that several different cell chemistries and types are subject to a wear-out-type of performance degradation. These curves are vertical translations of one another, differing only in the value of A as used in Eq. (1).

Since that time, cycle life data from a number of programs have become available. This information has been collected from various open sources and is shown in Figure 4. This figure represents the totality of cycle life data that was available as of the time of this writing. It represents information from different cell manufacturers, but no attempt has been made to identify them on the figure. Very often, due to the wide variation in the amount of excess capacity between different manufacturers, the DODs originally reported were adjusted so that all the cell types would have a 20% excess capacity at the start of cycling. The DOD values on this chart were based on the adjusted nameplate capacities.

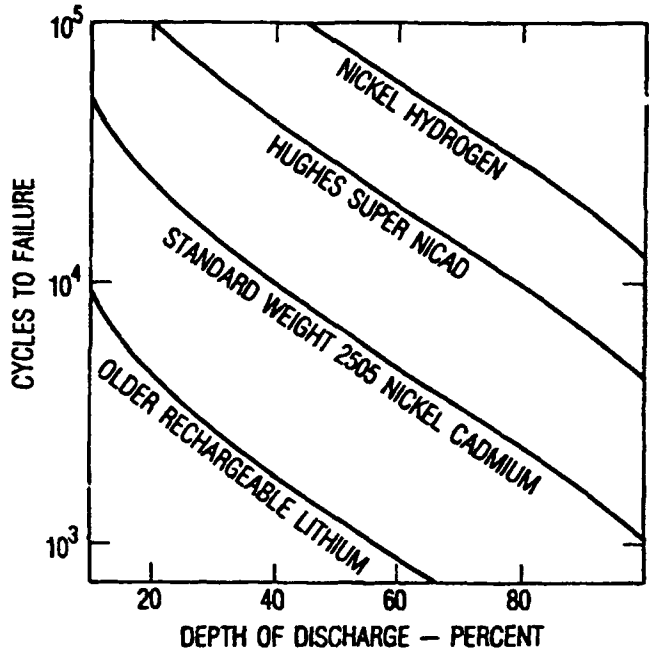

Figure 3. Cycle life prediction for several cell types

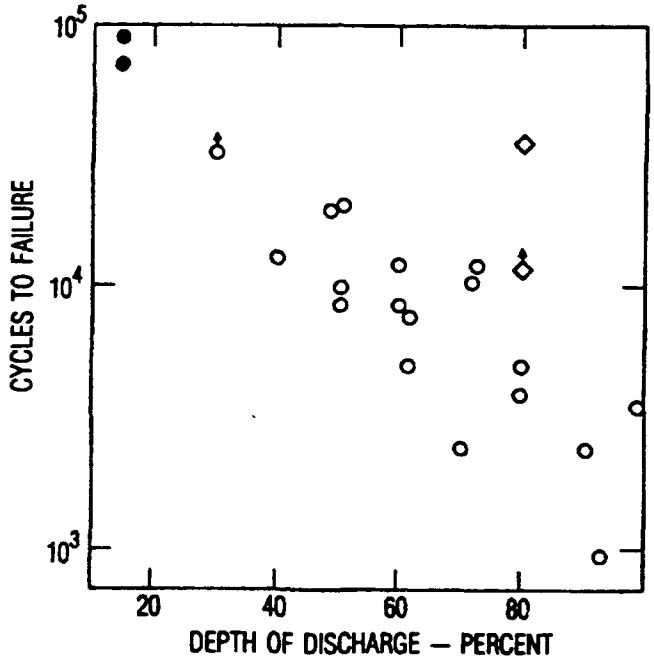

Figure 4. Compilation of nickel hydrogen life test data

All of the cells were 3.5 inches in diameter. Some of the cells had an electrolyte concentration of 38% KOH, while others used 31%, and a few (the diamond points) had 26%. The points with vertical arrows were still cycling as of this writing. The two solid circles are projected cycle lives based on capacity retention trends. The lower of the two diamond points for cells with 26% KOH illustrates the potential for superior cycle lives in aerospace cell hardware. The upper point was obtained from boiler plate hardware.

There are many more cells in several cycle life test programs that are still cycling. These data focus on cells that have come to the end of their useful service lives.

In general, the trend of the data is correct, but if the simple wear-out model would be valid, a better fit of the data to the model would be expected. The scatter or divergence is more pronounced at the deeper DODs. A typical cycle life vs DOD line cannot be positioned such that it fits the data very well. A more sophisticated model would be required to account for the large spread in cycle life at deep DODs.

Some relevant works of Fritts, Lim et al., and Davolio et al. are summarized in the following section as they relate to characteristics of cobalt-doped nickel active material in porous, sintered nickel plaque (Refs. 7–9). Their work related to different aspects of the expansion characteristics of nickel electrodes and how that affects their physical integrity. Space limitations permit only brief summaries of these efforts.

II. CHARACTERISTICS OF NICKEL ELECTRODES

A. Morphology Characteristics

Fritts carried out work that investigated the overall volume changes that took place within a sintered nickel electrode between the charged and discharged state (Ref. 7). Further, as a function of the percentage of cobalt addition, he measured a parameter that he called the strain of the electrode. This in turn was a function of the electrode hardness and its resultant expansion properties. Important variables included cobalt content and the loading level of the active material. The findings were striking in terms of the effect of cobalt additions on the amount of electrode expansion. Although there was little difference between the density of the active material in the charged and discharged state, the strain on the electrode structure was reduced by several orders of magnitude by the addition of about 10% cobalt. The amount of strain in these experiments is a function of the magnitude of force that the expanding active material exerts on the sinter structure of the electrode.

Expansion of the electrode can be undesirable for several reasons. First, it disrupts the dimensional characteristics of a stack of between thirty to fifty sets of repeating electrode, separator, and gas screen combinations which make up a typical cell assembly. These stacks of components are held under compression between spring mounted end plates. The permissible amount of travel in these springs, which can compensate for thickness increases of the nickel electrode, does not allow for a large increase in thickness of each electrode. Secondly,the expansion of active material within the porous structure that does take place, due to the density differences of the several species of active material present, can fracture the points of contact where the individual nickel particles are sintered together. This second effect results in a gradual reduction in the electrical conductivity of the electrode structure, leading to increased IR drop, as well as reduced utilization of active material. The author concluded that the reason for these results stemmed from the fact that cobalt additions to the active material significantly reduced its rigidity. For electrodes requiring longer cycle life at deeper DODs, this work would suggest that higher cobalt levels, lower loading levels, and a stronger starting plaque strength would be desirable.

Lim and Verzwyvelt also investigated the expansion characteristics of the active material within a nickel electrode using a different method (Ref. 8). They studied the "bending moment" of an electrode that had the electrode structure removed from one side of the perforated metal-foil current collector. With the expansion and contraction of the active material within this structure (Figure 5), a certain amount of bending took place. The effects of DOD, number of cycles, and lithium hydroxide were studied. Here too, the results were significant. Lithium hydroxide substitutions for potassium hydroxide resulted in reduced amounts of bending. The bending was found to be made up of a reversible and an irreversible component. Going through a complete cycle returned the electrode to almost its original position. Over a number of cycles, a gradual increase in permanent departure from its original vertical position was

noticed. This increased as the number of cycles, as well as the DOD, was increased. The loading level of active material used in this study was closer to the levels employed in aerospace nickel cadmium cells (about 2.0 g/cm^3 void) than the levels used in nickel hydrogen cells (about 1.6 g/cm^3 void). It was noted that, when lower loading levels were used, an "incubation" period of several hundred cycles was required before the effect seen with the higher loadings was noticed. In this study, longer cycle life would be suggested by lower DODs and additions of lithium hydroxide. However, lithium hydroxide additions introduce other complications and are not suggested for longer cycle lives in nickel hydrogen cells.

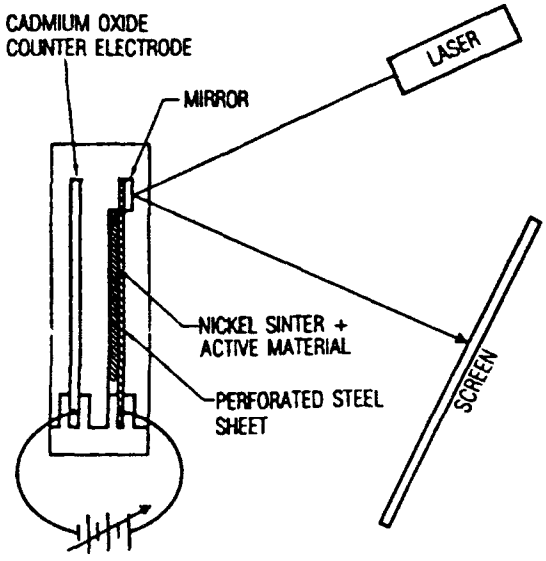

Figure 5. Schematic diagram of Lim's bending moment experiment

A valuable extension of the bending moment experiments of Lim is the flexural Young's modulus work of Davolio et al. (Refs. 9, 10). As with the two preceding studies, this work views the electrode structure as made up of two separate components. One is the rather soft matrix of sintered nickel particles when the active material is not exerting any pressure against the pore walls. Here, the mechanical properties are a consequence of plaque material. When the active material has expanded to the point that it begins to exert pressure against the pores within which it is contained, then the mechanical properties of the electrode structure change abruptly. Figure 6 shows the important details of Davolio's setup. The resistance to bending of an operating electrode is measured as it is being cycled. The variables being investigated in the work reported thus far include the DOD, concentration of potassium hydroxide, plaque material (foams, felts, sinters), loading level of active material, cobalt content, and method of cobalt addition. A major finding of his studies was that the electrode structure abruptly becomes stiff at a certain DOD. This stiffness increases until the end of discharge. Apparently the active material is expanding against and distorting the walls of the pore structure. At the very beginning of the next recharge, there is a rapid reduction in the electrode stiffness. The contracting active material mass must very quickly pull away from any compressive force against the pore walls of the plaque material. These studies are still ongoing and, thus, are

not complete enough to be able to fully understand the effects of all the variables of interest to aerospace-type nickel hydrogen electrode structures.

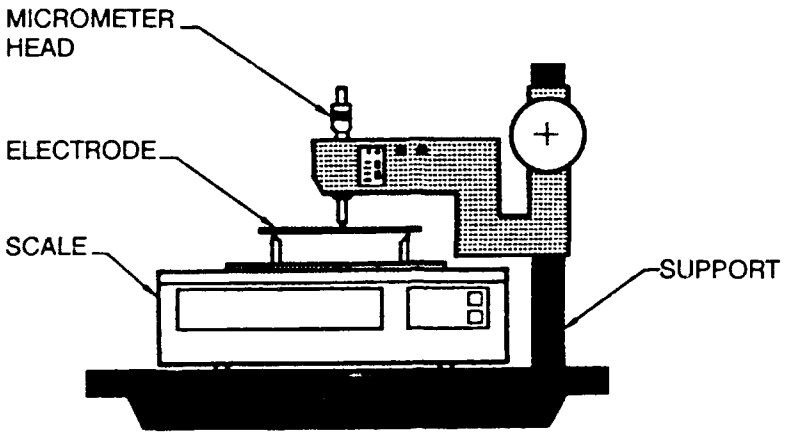

Figure 6. Schematic diagram of Davolio's flexural Young's modulus experiment

The following simplistic understanding of the nickel electrode represents a blending of the results of the three workers cited here, along with representative results from separate structural studies (Ref. 11). A significant finding of some of these structural studies states that the active material is seen as made up of platelets that are separated from one another by water, along with other ionic species, by distances that can range from 4.6 to 8.0 Å depending on the exact species present. These lattice constants are rather different from ones suggested from the classical values of the densities. As cycling takes place within a pore, there is a certain degree of expansion and contraction that accompanies these processes. There are two major considerations that come into play: (1) the magnitude of the expansions and contractions, which appears to be affected by the concentration of the potassium hydroxide, the DOD, the type and amount of additives (solid state or in solution), and possibly other factors, and (2) the impact of these expansions and contractions on the plaque structure. The cited studies have suggested the sinter strength, the loading level of active material, and its textural character to be the main contributors. Three cases can be postulated, and the following results might be expected over the cycle life of the electrode.

- Electrode lightly loaded, low concentration of potassium hydroxide, and low DOD cycling. Under this set of conditions, very little adverse effect of the expanding/contracting active mass on the plaque structure would be expected.

- Electrode heavily loaded, high concentration of potassium hydroxide, deep DOD, and high ratio of charge to discharge. This latter factor favors the formation of the gamma form of nickel oxyhydroxide. This structure has a very low density and, thus, exacerbates the expansion/contraction problem. Under this set of conditions, the active material would be expected to have adverse expansion effects on the plaque structure.

- Active mass in the form of a compliant, nonrigid structure. In this case the cycling mass would be able to adjust its shape to best fit the pore structure, or, if need be, extrude out of the pores without fracturing the plaque structure. This latter phenomenon was noted in the studies as reported in Ref. 2.

It is not fully understood where the boundaries are that separate the different types of interactions as listed above.

B. Modified Cycle-Life Model

The interaction of the active material with the nickel electrode plaque structure, as outlined in the preceding section, suggests a modification to the simple wear-out model. The collected cycle life data as presented in Figure 4 contained a large amount of variability at DODs beyond about 40%. Figure 7 presents the same data as shown in Figure 4 with a series of lines which were generated by assuming that there is an abrupt increase in the A factor as a result of the interaction of the expanding active mass with the plaque structure. Shown here are A factors that are increased by 2, 3, and 5 times as the DOD exceeds 40%.

The modified model will assume that, at the loading levels of active material generally used in nickel electrodes for nickel hydrogen cells, there is no excessive expansion of active material against the plaque pore structure at shallow DODs; or, the material is compliant enough that it can be accommodated. At some point (40% DOD was used in Figure 7) an increase in the

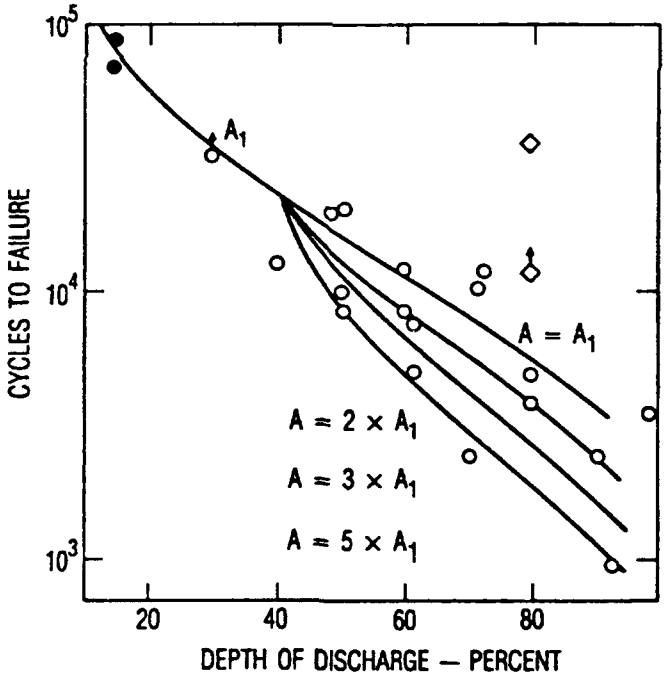

Figure 7. Cycle life prediction using the proposed modified wear-out model

rate of degradation takes place caused by the aforementioned factors. The amount of increase in the rate of degradation will depend on several factors, such as the cobalt level and probably the KOH concentration. That is the reason for the family of curves.

The work reported here explores this proposed model more closely using a method similar to that reported by Davolio. The depth of discharge at which the rate of change in electrode stiffness as a function of DOD increases is suggested as the point where an acceleration in the rate of capacity loss should take place. In this study, particular emphasis is placed on the effects of electrolyte concentration using typical electrode structures as used in nickel hydrogen cells. The results are then examined to see whether the suggested modified model is in agreement with this newer data.

III. EXPERIMENTAL SETUP

KOH solutions of 26%, 31%, and 36% were prepared from Baker analyzed grade reagents and distilled water. Precautions were taken to minimize the introduction of CO_2 during the preparation and use of these solutions. The electrochemical cell compartment was constructed of alkali-resistant polypropylene containers. Experiments were conducted at ambient room temperature (23°C) conditions.

The experimental apparatus is shown in Figure 8. A strain gauge mounted beneath a 1.6-mm-thick stainless steel support arm measured the load applied (g) to the nickel electrode specimen. A nickel rod 3.2 mm in diameter (99.99% purity) connected to the support arm was used to impinge upon the test specimen perpendicular to the nickel electrode surface. A programmable stepper motor provided precision displacement steps for the measurement of nickel electrode deflection (mm). Load and displacement measurements were independently calibrated using known reference values for the stepper motor and strain gauge. A PAR Model 173 potentiostat was used for galvanostatic control of the electrochemical cell during charge and discharge cycling.

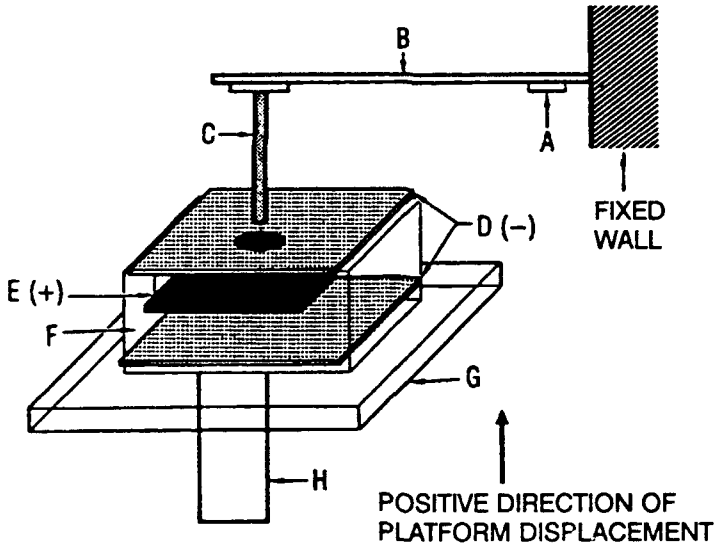

Figure 8. Schematic of experimental setup. (A) strain gauge, (B) support arm, (C) nickel rod, (D) Cd electrode, (E) nickel test electrode, (F) cell compartment, (G) support and stepper motor platform, (H) stepper motor displacement piston.

The experiments were carried out in the flooded condition in the appropriate electrolyte. Two porous cadmium electrodes (negative) and one nickel electrode (positive) test specimens were used in the single-cell design. The test specimen (6.5 cm^2 surface area) was placed sinter-side up facing toward the nickel rod load-measuring device. A 0.95-cm-diam hole was cut into the

top cadmium electrode to allow free access of the nickel rod to the nickel electrode. The test specimens were chosen from various nickel hydrogen cell nickel electrodes which had either been cycled or uncycled. These electrodes had known compositions of cobalt additives and levels of active material loading.

A single test run consisted of a continuous C/10 charge for 16 hr, followed by a C/10 discharge until the cell voltage reached a cutoff value of approximately 1.0 Vdc. In situ measurements of the nickel electrode load-displacement behavior were taken during the discharge portion of the cycling. These measurements were computer programmed to be taken every 1 hr from the beginning of the discharge (fully charged electrode) until the specified cell voltage cutoff value was achieved.

IV. RESULTS AND DISCUSSION

The results to date are limited to two types of electrodes, as described in Table 1. The electrode labeled Uncycled, was one that had received the usual number of cycles as per the manufacturing and activation procedure, but was never installed into an actual cell. The electrode labeled 1800 Cycles was from a cell that suffered capacity loss during storage and was subsequently cycled to failure. The electrode, when removed from the cell, was selected specifically because it had undergone considerable expansion during cycle life testing. Figure 9 shows a typical strength measurement for both the Uncycled and the 1800 Cycle electrode at 33% DOD. The zero of these measurement was taken as the point at which the applied load began to vary linearly with electrode displacement. This linear region of elasticity was used as a relative measure of the electrode modulus at a given DOD. These data were used to examine the structural changes occurring within the nickel electrode sinter structure as a result of active material expansion. Effects of the nickel electrode support screen on these measurements were considered negligible due to the small displacement (0.1–0.3 mm) of the electrode.

Table 1. Description of Electrodes Used in These Studies

Electrode	Uncycled	1800 Cycles
Plaque type	dry powder	dry powder
Cobalt level	about 10%	about 10%
Loading level g/cm^3 void	1.65	1.65
Impregnation type	alcoholic	alcoholic

Multiple test runs on each nickel electrode sample were conducted to establish the reproducibility of the data. The mechanical response of the electrode to an applied load was determined from the slope of the linear region of elasticity. Figure 10 shows the behavior of the uncycled nickel electrode tested in different concentrations of KOH. The steady increase in the relative electrode modulus with DOD suggests that the nickel electrode is becoming stiffer during cell discharge. These data also show a two-fold increase in stiffness from zero to full discharge independent of KOH concentration. This indicates that the mechanism for electrode swelling is limited by the state of charge of the active material. It should be noted that the uncycled electrode has not experienced the electrochemical environment of a nickel hydrogen cell. The weak dependence of KOH concentration on nickel electrode expansion has been observed by other investigators for heavily cycled (> 10,000 cycles) nickel hydrogen cells (Ref. 12).

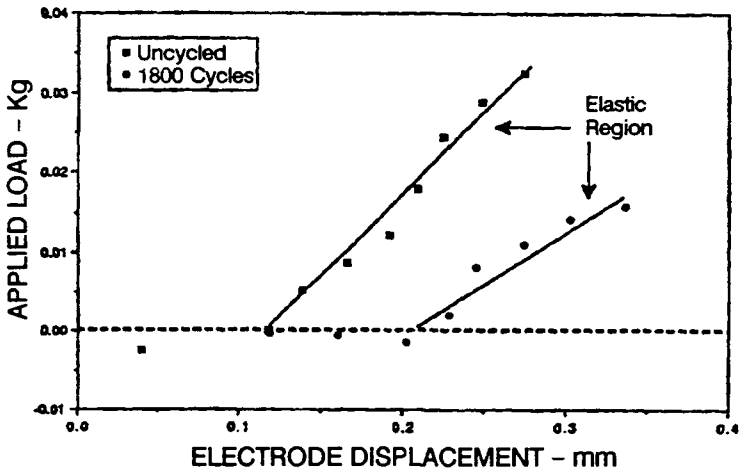

Figure 9. Typical nickel electrode strength measurements in 31% KOH and 33% DOD

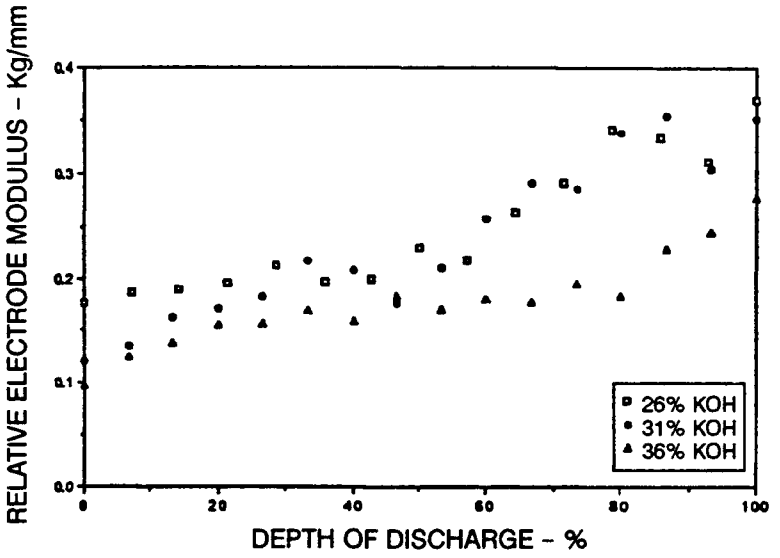

Figure 10. Effect of percent DOD on nickel electrode strength for an uncycled electrode at the C/10 discharge rate

It can be expected that similar measurements on electrodes from cycled cells will show degradation of the nickel sinter substrate that may result in a decrease in cell cycle life. Figure 11 shows these effects for the 1800-cycle nickel electrode. The initial slope of the electrode modulus with percent DOD is similar to that obtained for the uncycled electrode up to approximately 40% DOD. At this point a transition in the electrode sinter structure occurs, which causes an abrupt change in the electrode modulus with DOD. This transition may be due to the cumulative effect of expansion and contraction over the cycle life of the electrode, which

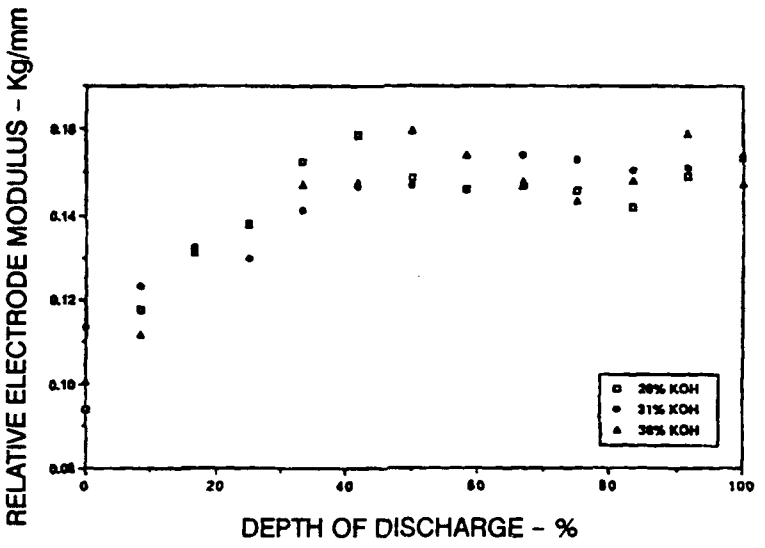

Figure 11. Effect of percent DOD on nickel electrode strength for the 1800-cycle electrode sample

forces the nickel sinter points to fracture and lose strength. The nickel electrode modulus remains at a constant value ranging between 0.14–0.16 (kg/mm) for the remainder of the discharge portion of the cycle. As with the uncycled electrode, the modulus of the 1800-cycle nickel electrode was independent of KOH concentration. These results suggest a dependence of nickel electrode swelling behavior on the cycle life history of the electrode and state of charge. Other cell variables such as cobalt additives, active material loading, and charge/discharge rate may also influence the mechanism for nickel electrode swelling.

V. CONCLUSIONS

A novel in situ method for the measurement of electrode strength has been used to examine the swelling characteristics of nickel hydroxide electrodes used in cells. These data have thus far shown no dependance of KOH concentration on the expansion behavior of the nickel electrode as a function of state of charge. However, cycle life history of the nickel electrode appears to govern the mechanical response of the nickel active material and sinter structure to DOD. The incorporation of these phenomena into the suggested modified degradation model will require further investigation.

REFERENCES

1. M. Oshitani, T. Takayama, K. Takashima, and S. Tsuji, *J. Appl. Electochem.* **16**, 403–412 (1986).

2. H. S. Lim, *Long Life Nickel Electrodes For Nickel Hydrogen Cells*, NAS interim report 3–22238 (September 1990).

3. L. H. Thaller and H. S. Lim, Paper 879080, *Proc. IECEC* (1987).

4. L. H. Thaller, *Expected Cycle Life vs. Depth of Discharge Relationships of Well Behaved Single Cell and Cell Strings*, NASA TM 82957 (1982).

5. *Accelerated Test Plan for Nickel Cadmium Spacecraft Batteries*, NASA Goddard Space Flight Spacecraft Center, Publication X–761–73–183 (October 1973).

6. H. S. Lim and S. A. Verzwyvelt, Paper 869367, *Proc. IECEC* (1987).

7. D. H. Fritts, *J. Electrochem. Soc.*, **129**, 118–122 (January 1982).

8. H. S. Lim and S. A. Verzwyvelt, Paper 859151, *Proc. IECEC* (1985).

9. G. Davolio, A. Pieve, and E. Soragni, *Proc. 16th Int. Power Sources Symposium*, Bouremouth, UK (September 1988).

10. G. Davolio, A. Pieve, and E. Sorangni, *Proc. Symposium Nickel Hydroxide Electrodes*, Hollywood, Florida, October 16–18 (1989).

11. J. McBreen, *Proc. Symposium Nickel Hydroxide Electrodes*, Hollywood, Florida, October 16–18 (1989).

12. H. S. Lim and S. A. Verzwyvelt, *Proc. Symposium Nickel Electrodes*, 341–355, October 16–28 (1989).

TECHNOLOGY OPERATIONS

The Aerospace Corporation functions as an "architect-engineer" for national security programs, specializing in advanced military space systems. The Corporation's Technology Operations supports the effective and timely development and operation of national security systems through scientific research and the application of advanced technology. Vital to the success of the Corporation is the technical staff's wide-ranging expertise and its ability to stay abreast of new technological developments and program support issues associated with rapidly evolving space systems. Contributing capabilities are provided by these individual Technology Centers:

Electronics Technology Center: Microelectronics, solid-state device physics, VLSI reliability, compound semiconductors, radiation hardening, data storage technologies, infrared detector devices and testing; electro-optics, quantum electronics, solid-state lasers, optical propagation and communications; cw and pulsed chemical laser development, optical resonators, beam control, atmospheric propagation, and laser effects and countermeasures; atomic frequency standards, applied laser spectroscopy, laser chemistry, laser optoelectronics, phase conjugation and coherent imaging, solar cell physics, battery electrochemistry, battery testing and evaluation.

Mechanics and Materials Technology Center: Evaluation and characterization of new materials: metals, alloys, ceramics, polymers and their composites, and new forms of carbon; development and analysis of thin films and deposition techniques; nondestructive evaluation, component failure analysis and reliability; fracture mechanics and stress corrosion; development and evaluation of hardened components; analysis and evaluation of materials at cryogenic and elevated temperatures; launch vehicle and reentry fluid mechanics, heat transfer and flight dynamics; chemical and electric propulsion; spacecraft structural mechanics, spacecraft survivability and vulnerability assessment; contamination, thermal and structural control; high temperature thermomechanics, gas kinetics and radiation; lubrication and surface phenomena.

Space and Environment Technology Center: Magnetospheric, auroral and cosmic ray physics, wave-particle interactions, magnetospheric plasma waves; atmospheric and ionospheric physics, density and composition of the upper atmosphere, remote sensing using atmospheric radiation; solar physics, infrared astronomy, infrared signature analysis; effects of solar activity, magnetic storms and nuclear explosions on the earth's atmosphere, ionosphere and magnetosphere; effects of electromagnetic and particulate radiations on space systems; space instrumentation; propellant chemistry, chemical dynamics, environmental chemistry, trace detection; atmospheric chemical reactions, atmospheric optics, light scattering, state-specific chemical reactions and radiative signatures of missile plumes, and sensor out-of-field-of-view rejection.